“Babeş-Bolyai” University of Cluj-Napoca,

Faculty of Chemistry and Chemical Engineering

CZIKÓ (căs. SÁRKÖZI) Melinda

“*Preparation, characterization and application of biocomposites”*

PhD thesis abstract

Scientific adviser:

Prof. Dr. DIUDEA V. Mircea

Cluj-Napoca

2015

"Babeş-Bolyai"University of Cluj-Napoca,

Faculty of Chemistry and Chemical Engineering

str. Arany János nr. 11, RO-400028, Cluj-Napoca

Scientific adviser

Prof. Dr. DIUDEA V. Mircea

Commitee members

President:

Prof. Dr. JANTSCHI Lorentz - Technical University of Cluj-napoca

Reviewers:

Prof. Dr. MUREŞAN Liana-Maria - Babeş-Bolyai University of Cluj-Napoca

Conf. Dr. BUNEA Andrea – University of Agricultural Sciences and Veterinary Medicine Cluj-Napoca

Conf. Dr. CLICHICI Simona – Iuliu Haţieganu University of Medicine and Pharmacy Cluj-Napoca

Public defense: **July 10, 2015**

Cluj-Napoca

2015

Acknowledgments

My doctoral research was financed from POSDRU/159/1.5/S/132400 - "Young successful researchers – professional development in an international and interdisciplinary environment" project of the Sectorial Operational Programme for Human Resources Development 2007-2013, co-financed by the European Social Fundand and Collegium Talentum.

Table of Contents (of the entire thesis)

Keywords: hydroxyapatite, carbon nanotubes, biopolymers, biocomposites, average particle size, sorption, *in vitro* testing

Introduction

Nowadays the preparation and amelioration of new composites is a very popular research area. The composite is a mixture of two or more different materials, which do not mix on micro level only on macro level, but they enhance the matrix material`s properties. *Biocomposites* belong to the group of composites, which preserve the biomaterial characteristics of the basic materials. Biocomposites are very important for the preparation of implants, which are used to improve integration with the surrounding tissues. Accordingly, hydroxyapatite (HAP), as basic material, is a good choice because it possesses high similarities to the mineral part of human bone. The disadvantage in using hydroxyapatite is that it has weak mechanical properties that can be improved with different additive materials. These materials influence the properties of the prepared materials. In this work silica, different biopolymers and –COOH functionalized multiwall nanotubes (fMCNT) are used as additives.

Silica was chosen because it has an essential role in the early stage of bone formation, without it bone deformation takes places. *Chitosan, polyvinilpirrolidone* and *gelatin* were added as biopolymers. These biopolymers are used also in tissue engineering, because of their influence on particle size variation. This way the specific surface area can be increased and finally the possibility of their application can be enlarged. By the addition of *carbon nanotubes* (CNT) the mechanical properties of the prepared composites are improved, because CNTs have unique mechanical properties.

The research work was elaborated to find adequate answers to the following *assumptions*:

1. Does the concentration of the precursors influence the reaction time and the particle size of the resulting materials?
2. Do different biopolymer additives influence the reaction time, the morphology and the particle size and thereby the specific surface area, which affects their sorbent properties and consequently their application?
3. Do the concentration of the added fMCNT and the preparation method of composites influence the properties of the prepared material?
4. Does the addition of chitosan to the fMCNT-HAP and fMCNT-HAPSi influence the properties of the resulting composites?

To find answers to these questions during the experiments the particle size variation in the process of synthesis and final particle size distribution, crystallite size calculations from X-ray diffraction data, thermal stability, morphology, sorption capacity and *in vitro* behaviour are studied.

I. Theoretical part

Biomaterials are nonviable materials used in medical and in other devices and they are intended to interact with biological systems. These materials are capable of getting in contact with the fluids and tissues of the body for a prolonged period of time, whilst eliciting little if any adverse reactions. Some biomaterials don't have suitable properties for application as bone graft materials but that can be improving by mixing with other materials.

Composite materials are formed of two or more constituent materials with significantly different physical or chemical properties, which when mixed result in a material with characteristics different from the individual components. The composite materials are formed by a *matrix* and a *reinforcement*. *Biocomposite* belong to the group of composites is a composite material which often mimic the structure of the living materials involved in the process keeping the strengthening properties of the matrix that is used, but always providing biocompatibility [1, 2].

Hydroxyapatite (HAP) is the basic material because this is the main inorganic component of bones and teeth. HAP has been extensively used as an implant material for bone substitute owing to its excellent osteoconductive properties [3-5]. The chemical formula of HAP is: $Ca_{10}(PO_4)_6(OH)_2$ [6] (Fig.1).

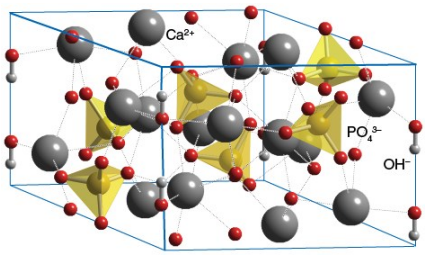

Figure 1. HAP structure

The application of hydroxyapatite as a substrate to stimulate bone ingrowth remains limited due to its extreme brittleness. *Silica* is known to be essential in the early stages of bone mineralization and soft tissue development [7] so, the structural modification of hydroxyapatite with silicon/silica is a great promise in the application of HAP as bone substituting material. Tissue engineering requires suitable biocompatible materials that can be used as scaffolds for the seeding with cells for the growth of a new tissue. It was found that nano structured

composites on the basis of biodegradable polymers and bioactive ceramics as HAP have the ability of stimulating the surface or chemical properties of the bone [8].

In order to achieve the highest efficiency for a specific application, it is essential to be taken into consideration the strong *relation between synthesis parameters* (precursors concentration, silica doping, bio-polymer addition, carbon nanotube addition) and *the characteristics* of the materials. Considering the above allegation, it is possible to control the final properties of HAP based materials together with their application by carefully choosing the synthesis parameters [9]. Hydroxyapatite applied in several fields, like in water purification [10-12], in adsorption chromatography for many years widely applied for separating various proteins as a column in a high performance liquid chromatograph apparatus separation [13, 14], substrates for drugs [15], catalysis [16] and the most important of these is application as biomaterial. In this case very important to know the response of reaction in the body. Appling HAP as implant material the first process after implantation is albumin adsorption on its surface [17].

The material properties (morphology, specific surface area, particle size, additive material) are of great influence on the sorption capacity. The sorption capacity and efficiency were studied for materials like betain [18], nicotinic acid [19] doxorubicin [20] and etc. [21-23]. In order to develop biomaterials with active substances that are dissolving at a specific rate optimal for the implant integration the sorption and desorption of inflammation reducing drugs (e.g. ibuprofen) is essential.

II. Experimental part

II.1 Preparation of materials

The experimental observations reported in several studies showed that nanocrystalline hydroxyapatite can be successfully prepared by the co- precipitation technique [24, 25]. Because of this the **co-precipitation** method is chosen for the preparation of HAP, HAPSi, CS/HAP, GEL/HAP and PVP/HAP materials. In the literature concerning the preparation of the carbon nanotube containing composites several different methods were presented. In this study three different methods: mechanical stirring (in ethanol), stirring in surfactant (Triton X) and co-precipitation method were used and the method resulting in the most homogeneous composites would be selected.

Hydroxyapatite preparation

HAP was prepared by co-precipitation method in controlled conditions [26] described by the following reaction:

$$\mathbf{10Ca(NO_3)_2 + 6(NH_4)_2HPO_4 + 8NH_4OH \rightarrow Ca_{10}(PO_4)_6(OH)_2\downarrow + 20NH_4NO_3 + 6H_2O} \qquad \mathbf{(1)}$$

The following materials were used as initial reagent: calcium nitrate tetrahydrate, diammonium hydrogen phosphate, 25% ammonia solution (Merck, Germany). The reaction time was 22 hours. After filtration the resulting materials were dried for 24 hours at 105°C (ncHAP). One part of materials was heat treated at 1000°C (cHAP). During the experiments three different initial precursor concentrations were used, to study the effect on the formation of the hydroxyapatite structure (*Table 1*).

Table 1. Initial concentration of precursors

Sample ID	$[Ca(NO_3)_2]_0$ (mol/l)	$[(NH4)_2HPO_4]_0$ (mol/l)
HAPI	1.5	0.9
HAPII	1	0.6
HAPIII	0.5	0.3

Silica substituted hydroxyapatite

HAPSi was prepared with the co-precipitation method in a similar way as hydroxyapatite; as SiO_2 source Na_2SiO_3 was used.

The substitution process of phosphate groups with silicate groups happened as follows:

$$Ca_{10}(PO_4)_6(OH)_2 + xSiO_4^{4-} \rightarrow Ca_{10}(PO_4)_{6-x}(SiO_4)_x(OH)_{2-x} + xPO_4^{3-} + xOH^- \quad (2)$$

The reaction time was 8 hours. After filtration of the resulting materials they were dried for 24 hours at 105°C (ncHAPSi). The heat treatment was performed at 1000°C (cHAPSi) [27].

Biopolymer-hidroxyapatite preparation

To the 0.09 or 0.45 wt.% chitosan or 0.5 and 0.1 wt.%GEL or PVP solutions were added drops of calcium nitrate and diammonium hydrogen phosphate solutions in order to obtain materials with different final biopolymer concentration. The synthesis time was 22 hour. After the reaction was accomplished, the precipitate was washed with ethanol and filtered. The filtered material was dried for 24 hours at 90°C [28].

Carbon nanotube-hydroxyapatite based composite preparation

Composites were prepared with three diferent methods: mechanical stirring in ethyl alcohol [29], mechanical stirring in Triton X [29] and co-percipitation method.

Co-precipation method

Beside the presented methods the composites were prepared also with chemical co-precipitation method [30]. As Ca^{2+} source calcium nitrate tetra hydrate and as PO_4^{3-} source di-ammonium hydrogen phosphate (Merck, Germany) were used. The calcium nitrate solution and carbon nanotube were stirred for 10 minutes for a better homogeneity. After that $(NH_4)_2HPO_4$ solution was added drop by drop to the reaction mixture. The reaction mixture pH was adjusted with the ammonia solution to the value of 11. The reaction time was 22 hours at room temperature. After filtration the precipitate was dried for 24 hours at 105 °C. The preparation of silica (10wt.%) containing composites was made in a similar way; Na_2SiO_3 being used as SiO_2 source [29], [31].

Preparation of CS-fMCNT-HAP and CS-fMCNT-HAPSi composites

The composites were prepared by co-precipitation method. In the first step –COOH functionalized multiwall carbon nanotube (fMCNT) was mixed with 0.5 mol L^{-1} $Ca(NO_3)_2*4H_2O$ and chitosan solution (1wt.%) with 0.3 mol L^{-1} $(NH_4)_2HPO_4$ solution were mixed for 10 minutes at pH=11 for the sake of good homogeneity. After the combination of

these precursor solutions the reaction mixture was stirred for 22 hours. To prepare 10 wt.% of SiO_2 containing composites Na_2SiO_3 solution was added together with $(NH_4)_2HPO_4$ solution.

II.2 Characterization of materials

Different characterization methods are used to determine the relationship between the structure of a material and its properties/applications. Depending on the characteristics of the investigated material, a suite of techniques may be utilized to assess its structure and properties. To investigate the new materials the following methods and apparatuses can be used. In the following the methods and the apparatuses used in this work are presented:

- morphology - transmission electron microscopy (TEM) and scanning electron microscopy (SEM)
- thermal stability – thermogravimetric analysis (TGA)
- particle size distribution - Shimadzu micro and nano particle size analyser
- crystallinity and structure - X-ray diffraction (XRD) and Infrared spectroscopy (FTIR)
- specific surface area - BET method

II.2.1 The formation of HAP structure and crystallite size of materials

The evolution of crystalline phases with reaction time was first studied from the XRD data. *Fig.2* shows the XRD patterns of hydroxyapatite synthesized at different synthesis times. The predominant phase was confirmed to be hydroxyapatite using ICDD standard no. 01-072-1243 [32]. The evolution of phase composition with reaction time showed that after 2 hours a poorly crystalline calcium phosphate phase was formed, which gradually transformed into HAP. As shown in *Fig.2* HAP was formed after 22 hours at all concentrations of calcium nitrate-tetrahydrate and diammonium hydrogen phosphate. Using different initial concentrations of precursors, no differences were observed in the crystallinity of the three samples.

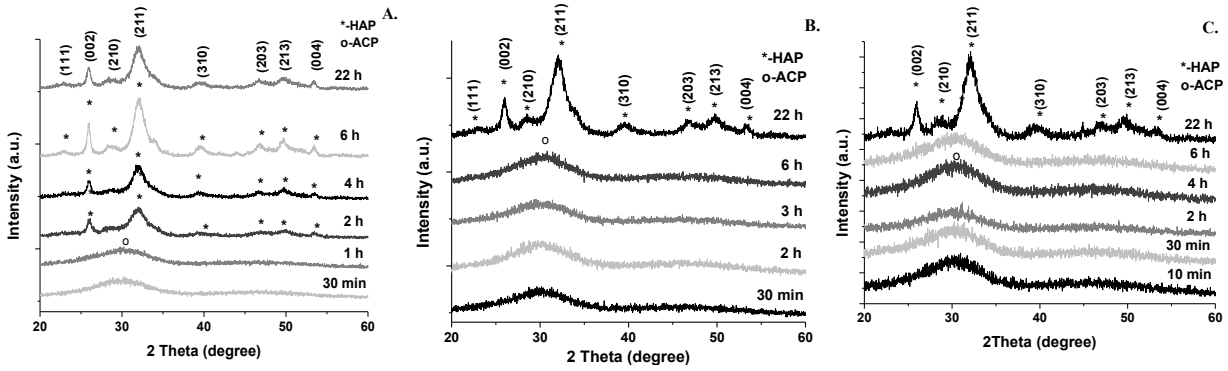

Figure 2. XRD patterns of **A.** HAPI, **B.** HAPII, **C.** HAPIII time series, formation HAP crystal structure during the synthesis

II.2.2 The effect of additive materials on the formation of hydroxyapatite crystal structure

The effect of polyvinylpyrrolidone (PVP) concentration variation

The XRD patterns of four PVP/HAP samples with various amounts of PVP are presented in *Fig. 3*. A single-phase apatite was observed in all four samples, and no secondary phase was detected by the XRD analysis. No major differences between the spectra were observed and the phase evolution in time was similar to HAP (*Fig. 2*). In all cases the PVP/HAP structure of hydroxyapatite was formed after 22 hours.

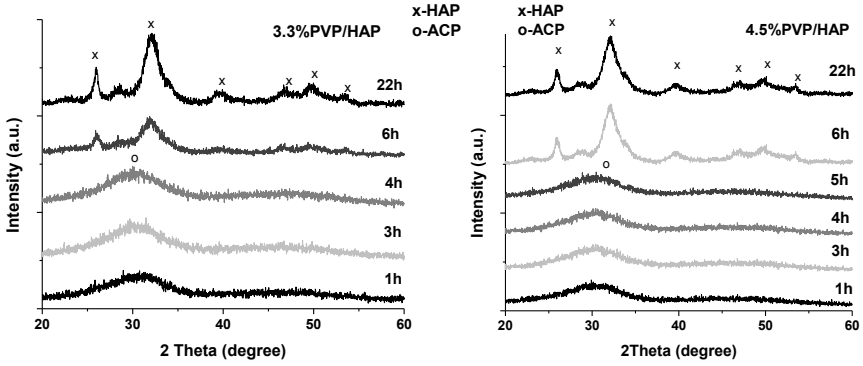

Figure 3. XRD patterns of 3.3%PVP/HAP and 4.5%PVP/HAP at different synthesis time

The effect of chitosan (CS) concentration variation

Fig. 4 shows the evolution of phases in time for CS/HAP samples with different concentration of chitosan. In case of 0.6%CS/HAP the evolution of phases showed a trend similar to that of HAP. However, by increasing the initial chitosan concentration in CS/HAP composites, an interesting phenomenon occurs. In alkaline conditions (pH=11–12), the formation

of unstable calcium phosphate (CaP) or amorphous calcium phosphate (ACP) phases occurred parallel with the appearance of crystalline HAP phase, which manifested as a fluctuation in time of the amorphous and crystalline phases during synthesis.

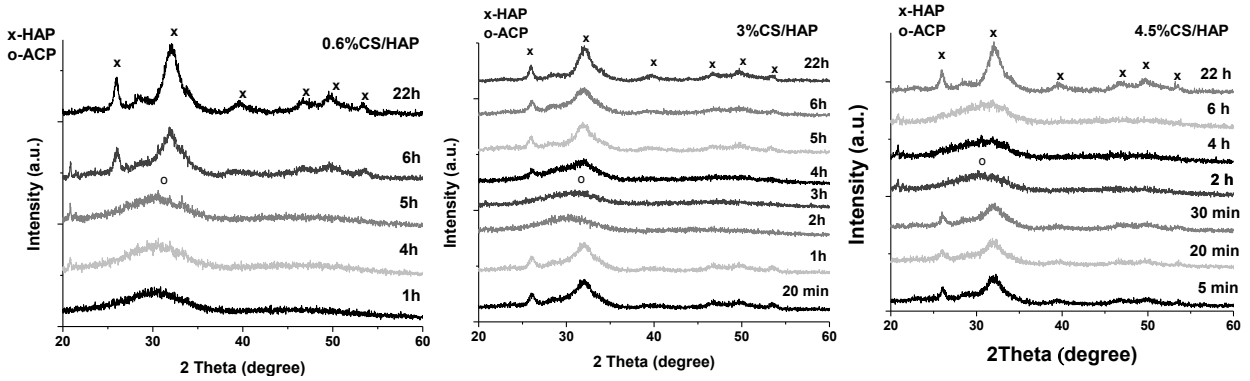

Figure 4. XRD patterns of CS/HAP composites at different synthesis time

At the beginning of the reaction a poorly crystalline phase [33] of calcium phosphate appeared and disappeared after 2 hours, and re-appeared at a different synthesis time. The transformation of these phases was completed in approximately 22 hours. It was during this period, most probably, that the HAP crystallites were formed from other CaPs phases. This indicates that CS had a chemical action, and not only a physical one. The poorly crystalline phase formation in the early stage of reaction could be explained by changes in the reactants` solubility due to the presence of chitosan. That interesting phenomenon was observed only after a certain CS concentration (< 1.6%) and could be explained by the complex phenomena that occur simultaneously in the reaction as precipitation and adsorption. Elucidation of the CS intercalation mechanism in this synthesis required further experiments.

Effect of carbon nanotube, silica and chitosan addition on the crystallinity of the composites

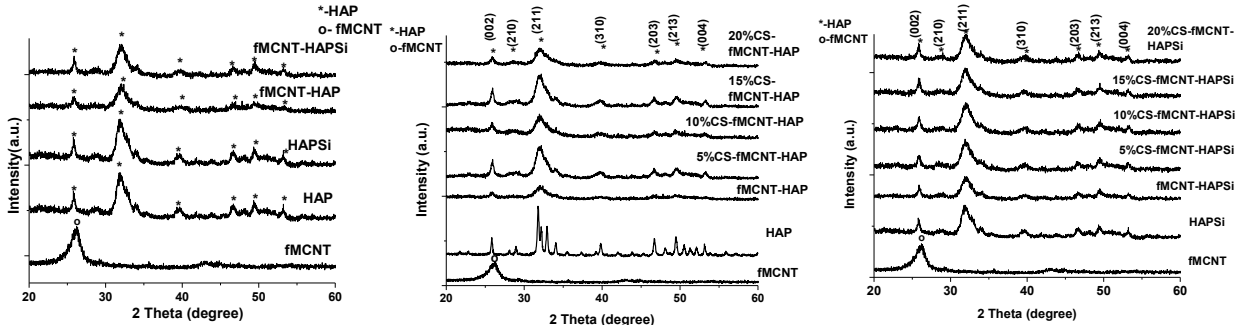

Figure 5. XRD patterns of fMCNT-HAP composites

The results are presented in *Fig. 5:* the XRD pattern of the fMCNT-HAP and fMCNT-HAPSi composites, with the inset of the pure fMCNT on the XRD diffractogram. No new peaks were observed for the fMCNT/hydroxyapatite composites and the 2Ɵ values were in agreement with those of pure HAP (ICDD standard no. 01-072-1243) [34, 35]. The peak of fMCNT was overlapping with the peak at 2Ɵ = 26 of the HAP. The substitution with silicon also did not appear to affect the diffraction pattern of the composites [36, 37]. The XRD pattern of the CS-fMCNT-HAP and CS-fMCNT-HAPSi composites are presented with the inset of the pure fMCNT on the XRD diffractogram. No new peaks were observed for the composites and the 2Ɵ values were in agreement with those of pure HAP [34, 38]. By adding fMCNT and chitosan to HAP the peak intensity decreased, which suggests a poorer crystallinity state [39, 40].

II.2.2. Determination of agglomeration tendency

Average particle size distribution and its variation during synthesis

The average particle size distribution and agglomeration tendency was determined with a Shimadzu SALD-7101 micro- and nano particle analyzer and a transmission electron microscope (TEM). The average particle size variation during synthesis of hydroxyapatite for three different initial precursor concentrations is represented in *Fig.6.A*. In the first six hours the average particle size gradually increased reaching the micrometer domain and after that it decreased. This phenomenon can be explained by the agglomeration and segregation of HAP particles while being prepared [28]. The lowest final particle size was in case of HAPII supposedly because the crystallite particle growth was suppressed in the favour of nucleation process (*Fig.6.A*). As additive materials polyvinylpyrrolidone (PVP) (*Fig. 6.C*), chitosan (CS) (*Fig. 6.B*), gelatin (GEL) and silica (SiO_2) were used. Macromolecules as additive materials act as a soft temporary template or nucleation centres to modulate the morphology of HAP [41, 42]. That is why the surface-regulating PVP was used as a capping agent to regulate the nucleation and crystal growth of HAP crystals. The change of size and shape of HAP nanocrystals, which were precipitated in an aqueous solution of PVP, related inversely to the polymer amount (*i.e.* the smallest particle size was observed with the highest PVP amount) [43]. In the PVP structure [44, 45] the O—H groups were located in abundance on the surface of HAP crystals, this was why hydrogen bonds could be formed between PVP and HAP, which prevented nanoparticle aggregation. So, the particle size in case of low polymer concentration was higher than in the case of pure HAP,

because the polymer promotes particle growth. At higher PVP concentration a larger number of reaction sites assured a higher number of HAP nuclei, and therefore a smaller particle size [43] - a growth-blocking action occurred. In the case of HAPSi and GEL/HAP the particle agglomeration process did not occur, the average particle size was constantly situated at the value of **16 nm**. From the 10 wt.% SiO_2 added to the HAP just 6.03% of that could be incorporated [27] and the remaining quantity of SiO_2 at alkali medium was polymerized [46] and formed a thin layer on the surface of the nuclei's and thereby inhibited their agglomeration. So silica inhibited crystal growth, and also reduced the agglomeration tendency [9]. For gelatin effect one explanation would be, the one published by Shu *et al.*[47] that its addition inhibits the nucleation, but also retarded the growth of the HAP crystals.

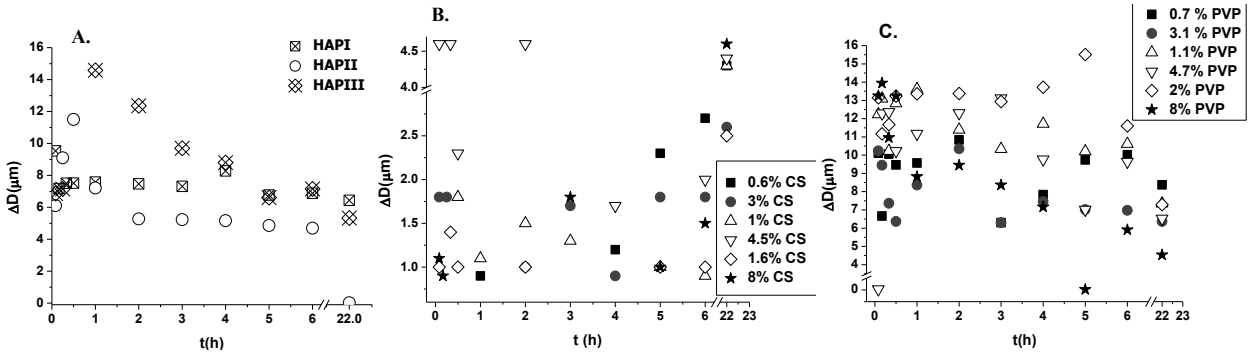

Figure 6. Particle size variation during HAP synthesis

By the addition of carbon nanotubes the particle size was decreased. The TEM images of HAP and CS/HAP nanoparticles indicate the formation of rod-like morphologies in all reaction conditions, whereas the PVP/HAP and the GEL/HAP presented a web-like structure. On the TEM images a homogeneous distribution of the fMCNT could be observed in powder phase. The highest homogeneity is found for materials with 10% CS and 10% fMCNT both for HAP and silica containing composites (*Fig.7*).

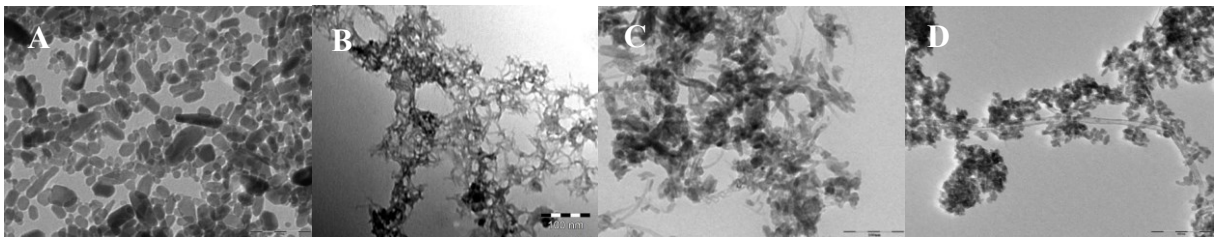

Figure 7. TEM images from A-HAP, B-1.1%PVP/HAP, C- fMCNT-HAP, D- 10%CS-fMCNT-HAP

II.2.3 Specific surface area measurements

Specific surface area and pore volume distribution were determined from the data of the N_2 adsorption-desorption isotherm conducted at 77 K. The specific surface area of HAP based materials with different fMCNT or/and polymer content were calculated with BET method and the pore volume distribution, as a function of pore diameter, with BJH method. The determination of the specific surface area is important for the evaluation of the chemical activity and sorption capacity of materials [48].

A good correlation could be noticed between pore volume and the specific surface area obtained for the materials with different additive content. The specific surface area was increased by the addition of SiO_2 (*Fig.8*) to hydroxyapatite and this effect can be re-found for polymer composites too. The highest specific surface area was determined in case of **2%GEL/HAP** because here the average particle size distribution was the smallest.

A good correlation can be noticed between pore volume and the specific surface area obtained for the materials with different fMCNT content. The specific surface area was increased by adding SiO_2 to hydroxyapatite. Also a specific surface area increase could be observed by carbon nanotube addition. The highest pore volume was measured for samples with 10% fMCNT (*Fig.9.B*). The relationship between specific surface area and pore volume was the following: the higher the specific surface area of the composites the more increased the pore volume is.

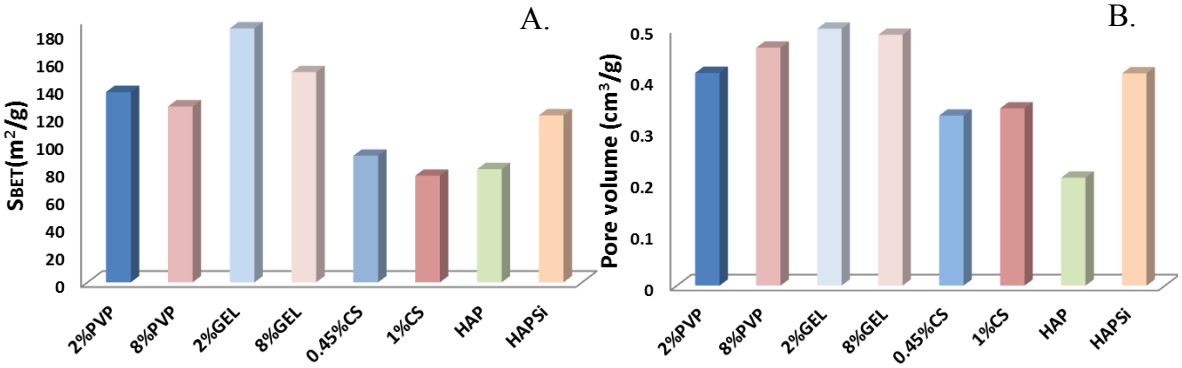

Figure 8. Specific surface area (A) and pore volume (B) of HAP, HAPSi and polymer/HAP materials

Fig. 9A and B evidences this relation, and highlights that composites with 10 wt.% fMCNT had the highest pore volume. Taking into account the data obtained for the specific surface area in function of fMCNT amount and its homogenous distribution in the HAP, we concluded that

further studies would be focused on composites prepared with co-precipitation method containing 10 wt.% fMCNT and the results presented in the following sections are for these composites.

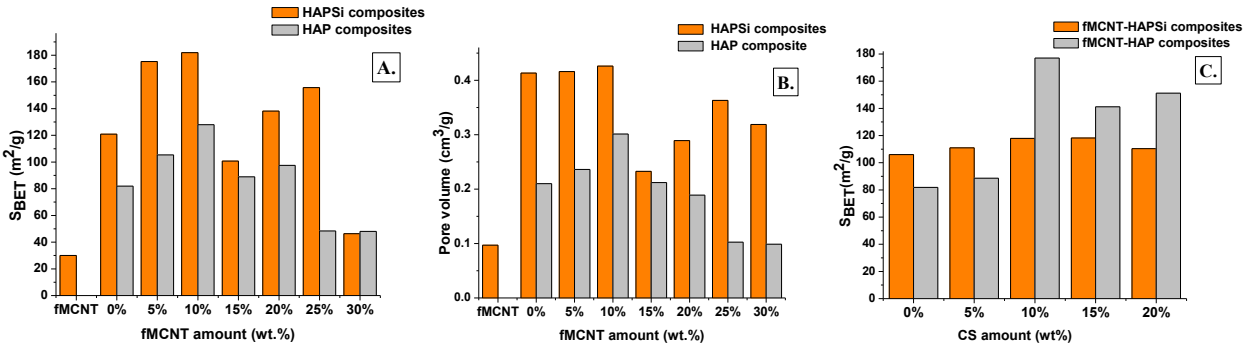

Figure 9. **A.** -Specific surface area, and **B.** -Porosity of HAP/HAPSi composites containing different amount of fMCNT, **C.**- Specific surface area in case of CS-fMCNT-HAP and HAPSi composites

In pure form, HAPSi had a higher specific surface (106 m^2/g) area than hydroxyapatite (81,9 m^2/g). The specific surface area of HAPSi composites was hardly influenced by the quantity of the added CS. In case of HAP composites the addition of polymer to the structure had a stronger influence to the specific surface area. The *10%CS-fMCNT-HAP composite had the highest specific surface area*.

II.2.4 *Thermal stability of the materials*

The thermal stability of the materials was determined by thermal gravimetric analysis (TGA). In addition, the differential thermogravimetric analysis (dTG) provides information about the way the organic part is eliminated, which depends on the degree of interaction between the hydroxyapatite and the additive materials [49].

The total weight loss in case of HAP and HAPSi could be divided in two-stages: between 30 –110 °C and between 200 – 500 °C. First the adsorbed water was eliminated from the surface and from the pores (~100 °C) [50], then at ~280 °C the decomposition of residual NH_4NO_3 and H_2O was performed, which were the by-products resulting from the synthesis reaction [51, 52]. By increasing the temperature a peak at 468 °C had been observed (*Fig. 10. A, B*), and the weight loss of 1.9% in case of HAP and 4.3% for HAPSi took place. These were the results of gradual dehydroxylation of HAP powder. This can be explained by the following reaction [53]:

$$Ca_{10}(PO_4)_6(OH)_2 \rightarrow Ca_{10}(PO_4)_6(OH)_{2-2x}O_x\square_x + XH_2O \quad (3)$$

In case of HAP at 468 °C the *x is 1.12* and 56.103% of –OH group was eliminated. This was calculated from the weight loss results accompanied with OH group elimination ratio.

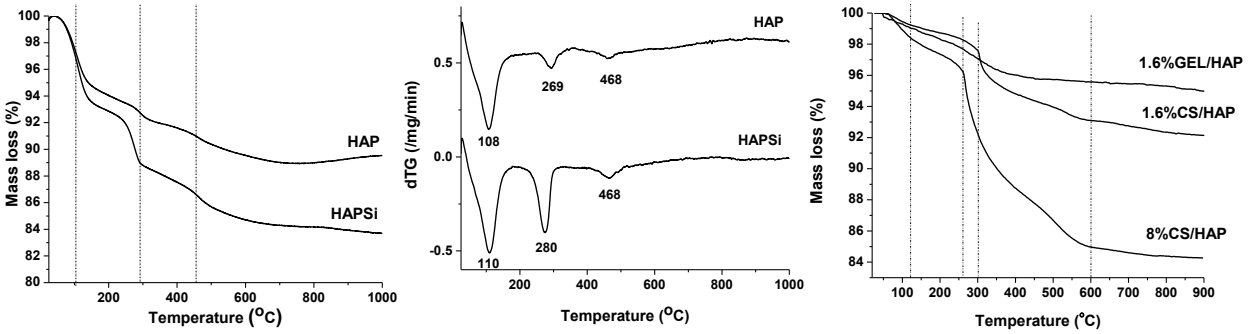

Figure 10. Thermal gravimetric analysis of HAP, HAPSi and polymer/HAP

In the case of gelatin containing composite at 320°C the thermal degradation and the pyrolysis of GEL molecules was taking place, and the peak about 430°C was associated with the final thermal degradation of the residual organics [54]. TGA studies of the composites containing chitosan showed three steps in weight loss. In the first step was eliberated the adsorbed water, in the second step at 280–300°C begins the degradation of the chitosan and in the third step at 500–610°C the whole quantity of CS was eliminated from the composites [55-57]. Before the thermogravimetric measurements the bio-polymer-HAP composites were ultrasonicated with ethanol and water for 6 hours for three times in order to eliminate the NH_4NO_3. This was the reason why the elimination of NH_4NO_3 was more reduced compared to the other materials (*Fig 10.C*).

For fMCNT the initial weight loss was 3.65% at 108°C due to the loss of adsorbed water [58]. Between 400°C and 600°C the elimination of fMCNT took place [59]. The highest weight loss was observed in the case of SiO_2 containing composites because the SiO_2 has a hydro binding effect. The TGA measurements show that the fMCNT-HAP composite had better thermal stability than fMCNT-HAPSi composites, because the elimination of fMCNT took place at higher temperatures (510-609°C), while in case of fMCNT-HAPSi this happened at 476°C. The silica group enhanced the interactions between -COOH groups of MCNT and OH groups of HAP, weakening the Van der Waals interaction in carbon nanotubes, resulting in decreased thermal stability [60]. The thermal stability of the composites was reduced by CS addition.

Decomposition of CS and elimination of fMCNT took place parallelly at the same temperature range.

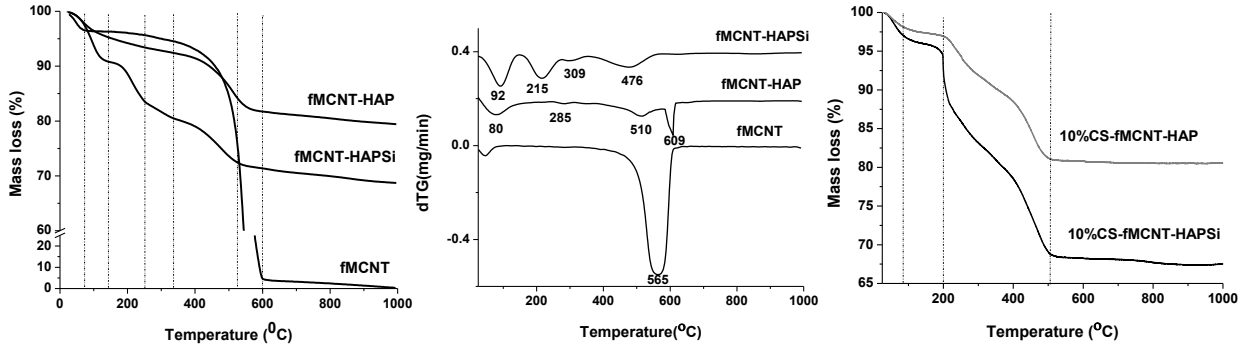

Figure 11. Thermal gravimetric analysis in case of fMCNT-HAP and CS- fMCNT-HAP composites

II.2.5 *In vitro* characterization of the hydroxyapatite based materials

Pure and silica doped hydroxyapatite and their gelatin, chitosan and carbon nanotube composites` biological activity were tested *in vitro* by studying their behaviour in simulated body fluid. The influence of heat treatment on pure hydroxyapatite, the effect of silica doping and bio-polymers addition, the immersion time and the form of the material (powder and compacted) was monitored and discussed. The materials were characterized pre-, during and post-SBF soaking by different methods. The results show that after 28 days of SBF soaking:

The materials had a better crystallized hydroxyapatite structure confirmed by XRD results, and in the case of gelatin, chitosan composites and silica doped hydroxyapatite a new phase appeared: $K^+$and Na^+ substituted HAP and respectively cristobalite for cHAPSi (*Fig.12*).

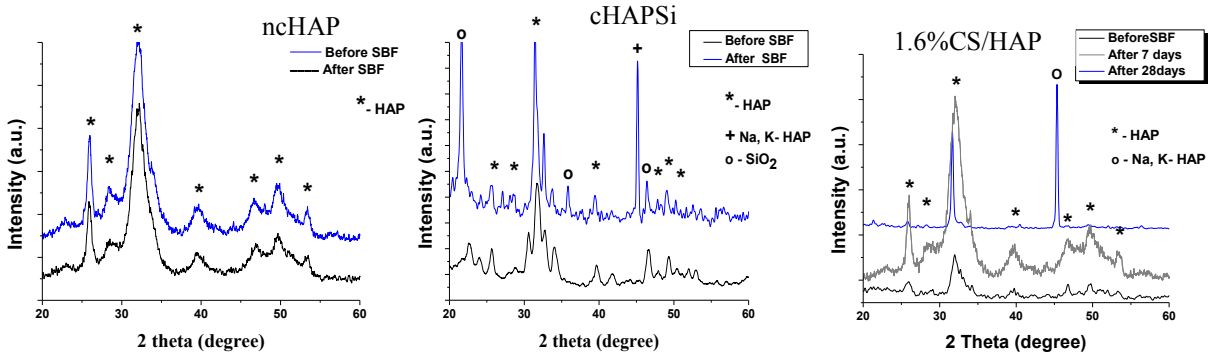

Figure 12. XRD spectrums of HAP and HAP based materials after (blue line) and before soaking in SBF solution (black line)

A new apatite bio-layer formation could be observed on SEM images which also was supported by FTIR spectra and TEM micrographs showed that hydroxyapatite and their composites were nano sized.

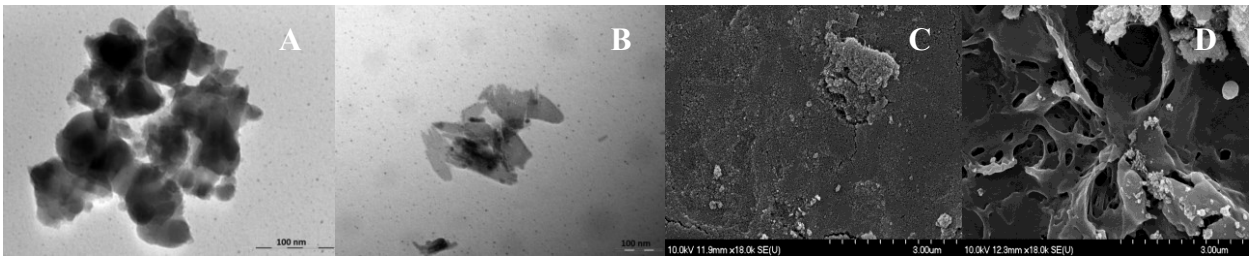

Figure 13. TEM imagines of **cHAPSi** before (A) and after (B) the SBF immersion and SEM imagines of **fMCNT-HAPSi** (C) and after (D) the SBF immersion

When the materials were incubated in SBF solution, the formation of apatite layer on the surface of pellet/powder went through a sequence of chemical reactions like spontaneous precipitation, nucleation and growth of calcium phosphate. It had been suggested that surface chemistry plays an important role in this process and even the functional groups of materials had a large effect on the bone-bonding property [61]. In order to demonstrate the formation of a new apatite layer the weight variation of the materials both in powder and pellet form was monitored. For all the materials, both in powder and pellet form, in the first 3-5 days a mass decrease (2-3 mass%) could be observed with further increase/decrease in the soaking time, suggesting a continuous precipitation of the bone-like apatite. The weight loss was more reduced for the chitosan and gelatin-hydroxyapatite composites, so the introduction of chitosan and gelatin increased the *in vitro* stability of the hydroxyapatite composites. Experimental results showed that after a 4 day immersion the weight of the pellets started to increase and continued to increase until day 28 (*Fig. 14*). This phenomenon was similar to the case of hydroxyapatite and hydroxyapatite with different additive materials. By adding carbon nanotubes both for HAP and HAPSi composites a decrease in hydroxyapatite layer formation during SBF soaking occurred.

The highest mass variation was recorded for cHAPSi, which showed a high mass loss in the first 3 days, but the final weight variation was above 4%. The chitosan and gelatin-hydroxyapatite composites were more stable, the weight loss was more reduced and the final mass variation was above 3.5%. This phenomenon supports that the introduction of chitosan and gelatin increased the *in vitro* stability of the hydroxyapatite composites. The average mass increase after 28 days was situated at for all materials between 3-4.5%.

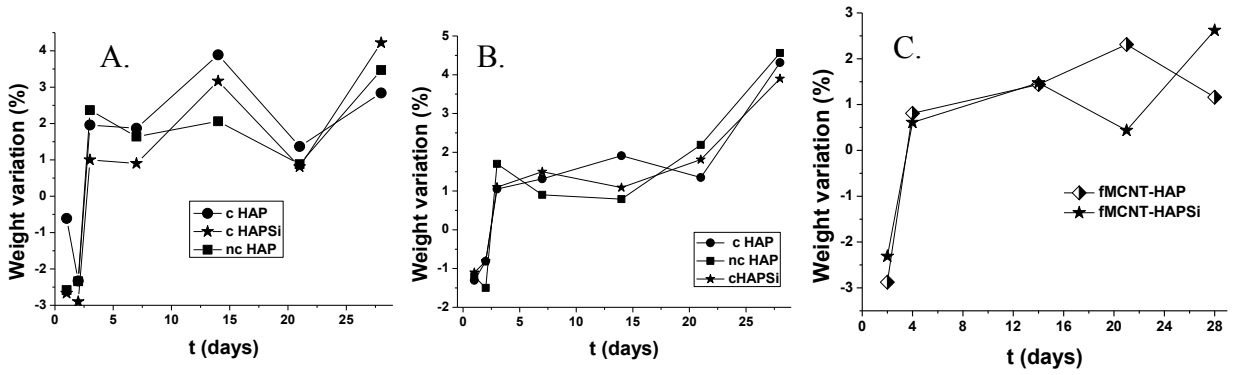

Figure 14. Weight variation of powder (A) and pellets (B, C) of HAP based materials in function of time during SBF soaking

Fig. 15 summarizes both for powder and compacted materials the final amount of calcium and phosphorus ions precipitated from the SBF. In the case of hydroxyapatite composite materials a much higher P ion consumption could be observed, compared to cHAPSi, non-calcined and cHAP. This can be explained by the formation of a larger quantity of Na^+ and K^+ ion substituted hydroxyapatite, which was supported by the XRD results. This suggested that gelatin and chitosan addition increased the ion exchange properties of the hydroxyapatite. P ion consumption was higher for the chitosan composites in the case of the pellets, and for the gelatin ones in the case of powder materials.For the heat treated hydroxyapatite also the P ion consumption was higher, and the amount of Ca^{2+} introduction in the newly formed bone-like apatite was small, which suggested a Ca-poor ACP formation tendency. On the contrary, for ncHAP and cHAPSi the Ca^{2+} consumption was high and the P ion was low, suggesting the precipitation of Ca-rich ACP in the first stage. Post-28 days of SBF immersion for all the materials a well crystallized bone-like apatite structure formation can be seen, as supported by the XRD results.

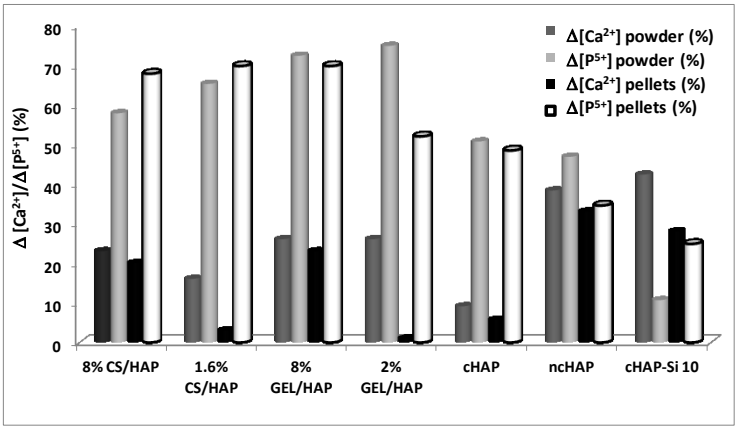

Figure 15. Calcium and phosphorous final ion concentration consumption in the case of powder and compacted HAP, HAPSi and biopolymer-HAP materials after 28 days SBF soaking

In case of fMCNT-HAP and fMCNT-HAPSi pellets *Fig. 16C* shows the changes in Ca^{2+} and phosphorous ion concentration variation in time during SBF soaking. The concentration of the ions oscillated in time. The Ca^{2+} and phosphorus ions were consumed from the initial SBF solution, which meant that the nucleation and growth of apatite outclasses the dissolution process [27, 46]. Until the 15th day the concentrations decreased, which is attributable to the formation of HAP, and then an increase was observed. These results were supported by the weight variation and by SEM measurements.

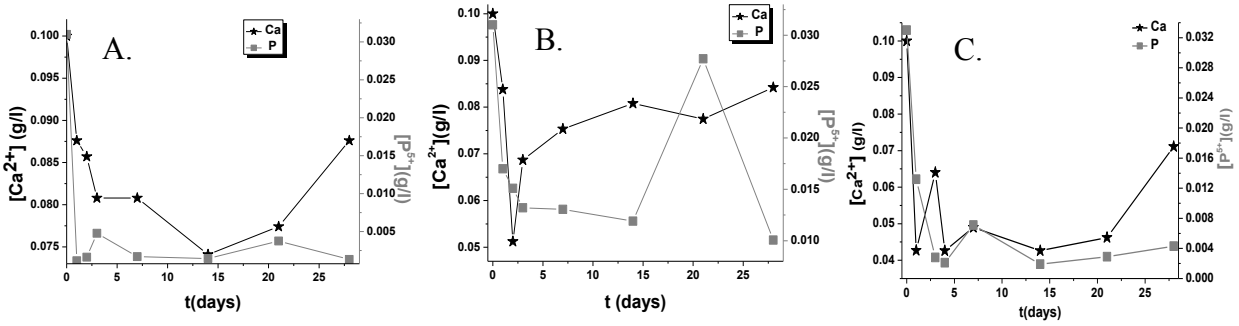

Figure 16. Calcium and phosphorous ion concentration variation of powder and pellet CS/HAP (A, B) and fMCNT-HAPSi pellet (C) in function of time during SBF soaking

Finally, comparing the powder materials to the compacted ones, it can be said that the powder materials were more soluble; in the first stage the dissolution of the materials was the predominant controlling step, which can be due to the higher specific surface area that increased

the chemical activity of the materials. All the materials promoted the formation of bone-like apatite on their surface; however the mechanism differed in function of the material phase composition and their form: powder or green compacts.

III. The application of hydroxyapatite based composites as substrates in different sorption processes

III.1 Albumin sorption

It is important to study the albumin sorption because after implantation proteins make the connection between organic and inorganic phases [62].

Bovine serum albumin (BSA) in our study was used as a model protein to determine the *sorption efficiency* and *capacity* CS-fMCNT-HAP and CS-fMCNT-HAPSi composites with different chitosan content. Hydroxyapatite had a multiple site binding character for proteins, a Ca^{2+} and a P site, that was why HAP gains a good protein bonding ability [63]. The bonding ability became better if the number of bonding sites were increased, the addition of –COOH functionalized carbon nanotubes and chitosan. Hydrophobicity of individual BSA and of the composite molecules enhanced their mutual interaction and sorption behavior. The foremost role for surface sorption was governed by the electrostatic force of attraction between BSA and HAP, in the case of pure hydroxyapatite. The sorption phenomenon of BSA on HAP nanoparticles was attributed to electrostatic interaction between Ca^{2+} cation and PO_4^{3-} anion of HAP nanoparticles with COO^{-} anion and NH_4^{+} cation of BSA protein [17, 64]. BSA was sorbed mainly through electrostatic attraction between the COOH group of BSA and the calcium ion exposed to an ion exchange on the surface of HAP [65]. The amount of protein sorption depended on the specific surface area, surface charge density, and pore size distribution [66].

In *Fig. 18* the sorption efficiency and in *Fig. 19* the sorption capacity were showed for 1 and 0.5 g/l initial BSA concentration in 7,5 and 8 pH TRIS based buffer. The reason to study for two different pH was motivated by the statement, that the lateral repulsion between the protein molecules was more significant at higher solution pH, which also played a role in lower sorption [67]. Our findings support the literature data, the sorption efficiency at pH=7.5 was more efficient than at pH=8, so by increasing the pH value the sorption efficiency decreased. Comparing hydroxyapatite with silica substituted hydroxyapatite the former had a higher sorption capacity and efficiency, this result being in accordance with specific surface area measurements.

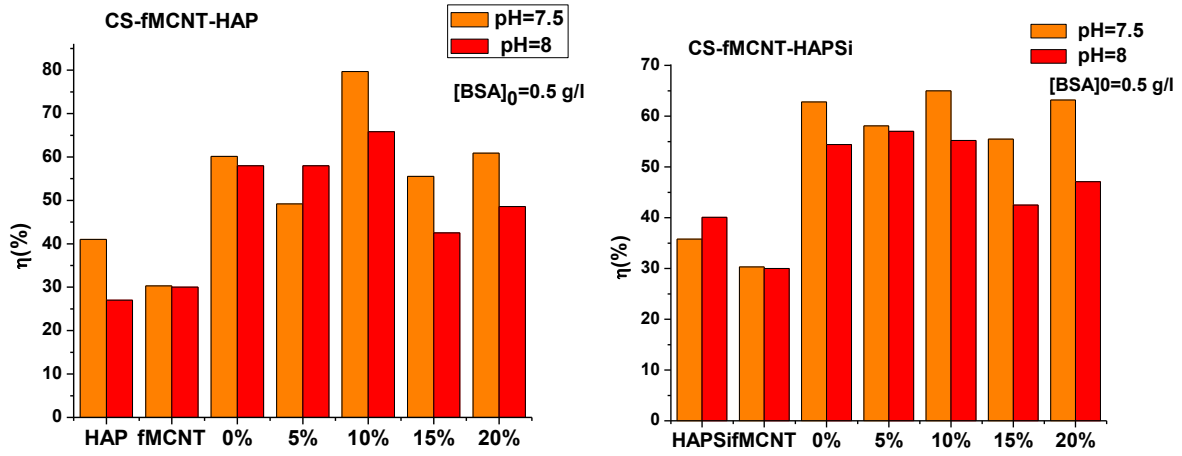

Figure 18. BSA sorption efficiency of CS-fMCNT-HAP/HAPSi composites in two different pH

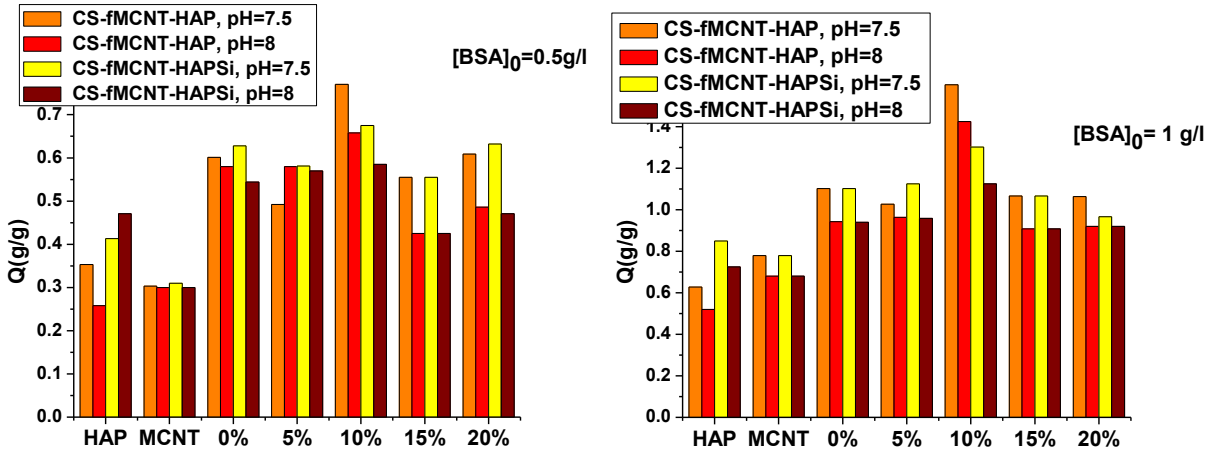

Figure 19. The BSA sorption capacity of CS-fMCNT-HAP/HAPSi composites

In *Fig.20* was shown the sorption capacity variation of 5%CS-fMCNT-HAP and 5%CS-fMCNT-HAPSi at pH=7.5 and 0.5g/l BSA concentration during the sorption process. During the measurements the sorption capacity showed a fluctuation caused by the "competition" between sorption and desorption till the equilibrium was reached; this is a characteristic property of nanomaterials [68].

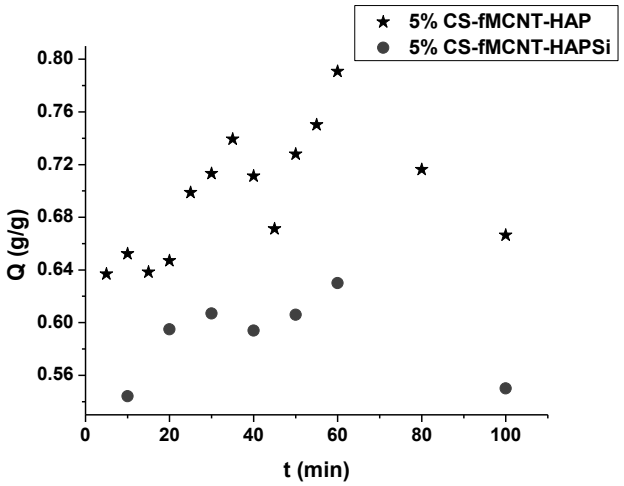

Figure 20. BSA sorption in time, $[BSA]_0$=0.5 g/l, pH=7.5 in case of 5%CS-fMCNT-HAP/HAPSi

In Fig. 19 was clearly showed that 10%CS–fMCNT–HAP had the highest sorption capacity at pH=7.5. Thus on this composite was determined the maximum sorption capacity in the range of 0,2 – 2,5 g/l initial BSA concentration at 7.5 pH. The maximum sorption capacity was at 2 g/l initial BSA concentration; in case of higher initial concentrations the sorption capacity was not increasing, so the maximum sorption capacity remaines ~ 1,6 g/g.

III.2 Ibuprofen sorption

Ibuprofen (IBU) was used as the model drug for studying the sorption and desorption capacity of composites and hexane was used as a solvent for ibuprofen [69]. UV spectroscopy indicated that the optimal wavelength for determining the loading and released of ibuprofen in hexane and in SBF, which was about 272 nm. A series of calibration solutions were prepared, containing 0.811 to 0.18 g/L of ibuprofen in hexane and their UV absorbance was measured, giving a linear plot of absorbance against ibuprofen concentration with an R^2 factor of 0.977.

The sorption capacity increased up to 17 g/l initial IBU concentration, after that the capacity did not increase. The composite sorption capacity reached its maximum and could not sorbed more. Thus for further measurements the 17g/l as initial IBU concentration was used.

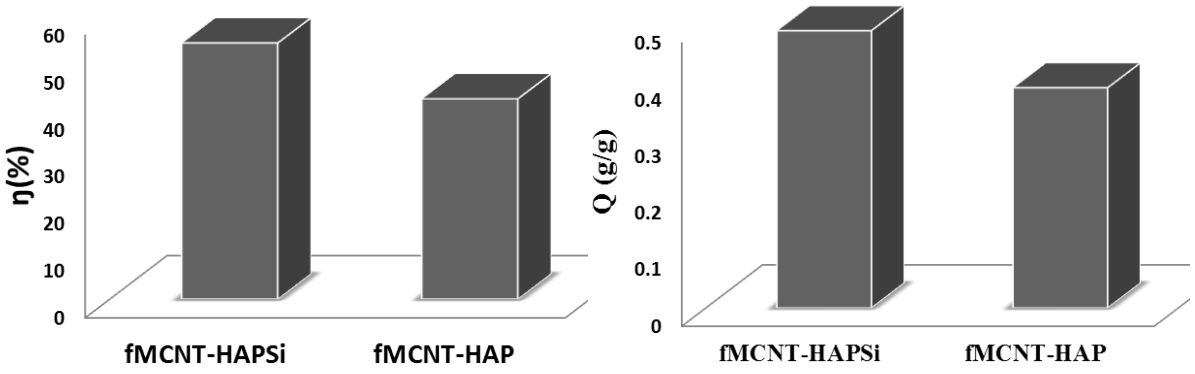

Figure 21. IBU sorption capacity and efficiency of composite

The literature presents two hypotheses for IBU sorption: (i) pores could be progressively filled up to a threshold for which the whole porous volume would be completely saturated, and the additional ibuprofen could only be deposited onto granules; (ii) the granule surface could first be coated with the drug substance, and pores would be progressively filled by the increase of the deposited quantity [70]. The sorption capacity and efficiency in case of composite with silica was higher (with more than 100 mg/g) than for the composite without silica (*Fig. 21*). This could be induced by the higher specific surface area of the composite with silica.

III.3. Ibuprofen desorption

Ibuprofen release was carried out by immersing the samples into simulated body fluid in pelleted form. The desorption of IBU from the composites was a good possibility for revealing its retard effect. Comparing the two composites, the one containing silica had a longer ibuprofen dissolution time. E. Chevalier *et al.* states that the intrusion of ibuprofen into the pores is correlated to the higher porosity of composites [70], which leads to a lower surface content. In our case this could cause a longer ibuprofen release time for the fMCNT-HAPSi composite (*Fig. 22.B*). For fMCNT-HAP the whole quantity of sorbed IBU was desorbed after 57h, and the half of this quantity was desorbed during the first day (*Fig.22*). In case of fMCNT-HAPSi in the first 24 hours just a small percent (11%) of IBU desorbed, than after 48 hours the desorption accelerated. After 57 hours 50% of the sorbed quantity of IBU was desorbed, compered to the fMCNT-HAP composite, where for this interval the desorption was completed. As the sorption also the release of IBU was expected to be governed by two different way, one of these was the diffusion process [71]. In this case the solvent enters the composite pores, IBU was then slowly

dissolved into SBF from the surface and diffuses from the system along the solvent-filled pores. The other way was controlled by forming hydrogen bonds with the carboxyl group of IBU when IBU was sorbed on the surface [72]. The desorption from the silica containing composite was slower than in case of composites without silica, because the number of hydrogen bonds were higher. Silanol groups from the surface and in the pores were thought to have an impact on the ibuprofen drug loading, because of the pharmaceutical interaction via hydrogen bonds with surface silanol groups [73].

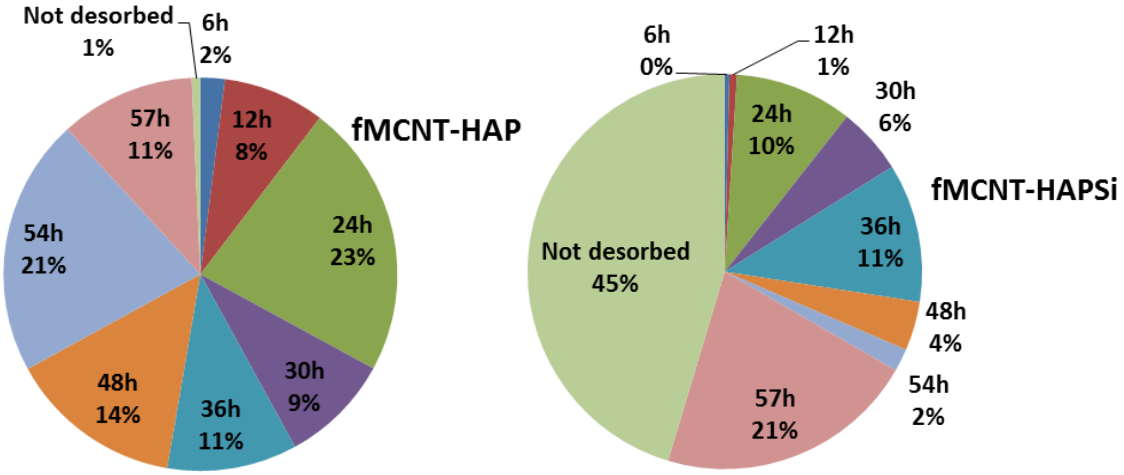

Figure 22. IBU desorption efficiency in time

IV. General conclusions

The thesis presents the *preparation, characterization and possible applications* of hydroxyapatite based biocomposites. The selected basic material was hydroxyapatite, which is the main inorganic component of bones, thereby it has a very good biocompatibity and bioactivity, but has weak mechanical properties that can be improved by additives. Hydroxyapatite based materials have a variety of applications, therefore it was important to study their preparation conditions and their properties, because these and the application fields are strongly related.

During the experiments the effect of these additives was studied with several material characterization methods. The thesis has two important parts, the division was made according to the type of the used additives: A- silica and bio-polymers: chitosan (CS), polyvinilpirrolidone (PVP), gelatin (GEL); B- COOH functionalized multiwall carbon nanotube (fMCNT) and chitosan; their effect on the properties of the prepared material was discussed. During the

experiments the following were studied: *reaction time variation in function of precursor concentration; average particle size distribution; crystallite size; crystallinity; thermal stability; morphology; sorption capacity; in vitro behaviour.*

A. The effect of the added SiO_2 and biopolymers on the prepared materials properties are the following:

1. The *co-precipitation method* was chosen for the preparation of materials. The *reaction time was reduced* by increasing the concentration of the precursors (22h→6h) or by the addition of more than 1.6 wt.% chitosan.
2. The crystallite size of polymer/HAP powders were smaller than pure HAP ones. The effects of CS and PVP were different, the formal reduced (43→46 nm) and the latter increased (62→90 nm) the size of the crystallites.
3. The results of *particle size distribution* and *specific surface area* measurements were *correlated* with each other, the materials with small particle size had high specific surface area; the GEL/HAP had the smallest particle size and the highest specific surface area.
4. The thermogravimetric measurement (TGA) and XRD measurement both suggested that during the heat treatment the HAP structure did not decompose below 1000°C. On the TGA curves 3 different phases could be distinguished: in the first step the adsorbed water, in the second step the by-product (NH_4NO_3) and in the third step the water was eliminated from the HAP structure.
5. For the *in vitro* testing the materials were immersed in simulated body fluid, during the soaking a new apatite layer was formed on the surface and the material crystallinity was increased. In case of additives-hydroxyapatite materials a *new* Na^+/K^+-HAP *phase* formed. During the immersion all material weight increased, but in case of GEL/HAP and CS/HAP the rate of weight increase was the highest (<4.5%, while HAP had >4.5%).

Based on these results the nano-form application of these materials is recommended, for example, in applications such as drug carriers or as sorbent materials in water purification.

B. The effect of added SiO_2, chitosan and multiwall carbon nanotube on the prepared composites:

The main role of the carbon nanotube addition is to enhance the mechanical properties of the composites.

1. The optimal fMCNT content was *10wt.%*, and the optimal method was the *co-precipitation method* because in these cases the composites had the highest homogeneity and the highest specific surface area.
2. Crystallinity was reduced by the addition of fMCNT and CS to the HAP, but the characteristic peaks were still to be observed.
3. It was found that combining –COOH functionalized multiwall carbon nanotubes with hydroxyapatite, containing different concentration of chitosan, and/or 10 wt.% silica, materials with *10 wt.% CS* had the highest homogeneity and the highest specific surface area.
4. When both chitosan and silica were present in the structure of HAP, the specific surface area did not change significantly with the increase of chitosan content. But in the absence of silica in the composites, the specific surface area also increased with the increase of the initial concentration of the CS.
5. The combustion of carbon nanotubes took place at a lower temperature in case of fMCNT-HAP and fMCNT-HAPSi composites compared to the decomposition temperature of the pure fMCNT. The fMCNT-HAPSi had a lower thermal stability than fMCNT-HAP. The thermal stability of the composites was reduced by CS addition. Decomposition of CS and fMCNT took place parallel.
6. Addition of fMCNT to HAP influenced the properties of the materials. *In vitro* bioactivity tests suggested that, fMCNT reduced the amount of new HAP layer formation during SBF immersion.
7. In revealing their applicability *as drug support* materials the sorption capacity and efficiency was determined by studying the sorption of albumin and ibuprofen. Comparing the sorption capacity of HAP, fMCNT and CS/fMCNT-HAP/HAPSi materials it was found that the *BSA sorption efficiency at 7.5 pH* was more efficient than at pH=8. Composites without silica have a higher sorption capacity and efficiency than those with silica and this was correlated with the specific surface area measurements.

8. In the case of ibuprofen sorption, the composite with silica had the highest sorption capacity and efficiency, and the desorption of IBU had a retard effect, after 57 hours just 55% of IBU was desorbed, while in case of materials without silica the whole IBU quantity was desorbed.

The added carbon nanotubes, in base of literature, enhance the mechanical properties of the resulted composites, but measurements of mechanical properties of these composites containing fMCNT is a future plan.

This thesis presented and supported the fact that material properties are influenced by the preparation conditions and their applications implicitly. The prepared hydroxyapatite based materials are suitable to use them as *drug carriers.* The aim of drug carriers is to achieve a controlled and slow release rate of the drug in order to insure a constant *in vivo* drug concentration for a longer period of time and to prevent harmful side-effects [74-76]. The specific application of these materials as drug carriers requires additional studies.

Selected bibliography

1. F. Xie, E. Pollet, P.J. Halley, L. Avérous, Starch-based nano-biocomposites, Progress in Polymer Science, 38 (2013) 1590-1628.
2. D.L. Batchelar, M.T.M. Davidson, W. Dabrowski, I.A. Cunningham, Bone-composition imaging using coherent-scatter computed tomography: Assessing bone health beyond bone mineral density, Medical Physics, 33 (2006) 904.
3. N. Rameshbabu, K.P. Rao, T.S.S. Kumar, Acclerated microwave processing of nanocrystalline hydroxyapatite, Journal of Materials Science, 40 (2005) 6319-6323.
4. N. Pramanik, S. Mohapatra, P. Bhargava, P. Pramanik, Chemical synthesis and characterization of hydroxyapatite (HAp)-poly (ethylene co vinyl alcohol) (EVA) nanocomposite using a phosphonic acid coupling agent for orthopedic applications, Materials Science and Engineering: C, 29 (2009) 228-236.
5. Z.-H. Zhou, P.-L. Zhou, S.-P. Yang, X.-B. Yu, L.-Z. Yang, Controllable synthesis of hydroxyapatite nanocrystals via a dendrimer-assisted hydrothermal process, Materials Research Bulletin, 42 (2007) 1611-1618.
6. L. Hao, H. Yang, N. Zhao, C. Du, Y. Wang, Controlled growth of hydroxyapatite fibers precipitated by propionamide through hydrothermal synthesis, Powder Technology, 253 (2014) 172-177.
7. N. Hijon, M. Victoria Cabanas, J. Pena, M. Vallet-Regi, Dip coated silicon-substituted hydroxyapatite films, Acta biomaterialia, 2 (2006) 567-74.
8. A. Rogina, M. Ivankovic, H. Ivankovic, Preparation and characterization of nano-hydroxyapatite within chitosan matrix, Materials science & engineering. C, Materials for biological applications, 33 (2013) 4539-44.
9. E.S.B. Melinda Czikó, Mircea Vasile Diudea, Reka Barabas Research on hydroxypatite based composite materials, Revue Roumaine de Chimie, 59 (2014) 353-357.
10. A. Corami, S. Mignardi, V. Ferrini, Copper and zinc decontamination from single- and binary-metal solutions using hydroxyapatite, Journal of hazardous materials, 146 (2007) 164-70.
11. J. Reichert, J.G.P. Binner, An evaluation of hydroxyapatite-based filters for removal of heavy metal ions from aqueous solutions, Journal of Materials Science, 31 (1996) 1231-1241.
12. C. Stotzel, F.A. Muller, F. Reinert, F. Niederdraenk, J.E. Barralet, U. Gbureck, Ion adsorption behaviour of hydroxyapatite with different crystallinities, Colloids and surfaces. B, Biointerfaces, 74 (2009) 91-5.
13. K. Kandori, A. Fudo, T. Ishikawa, Adsorption of myoglobin onto various synthetic hydroxyapatite particles, Physical Chemistry Chemical Physics, 2 (2000) 2015-2020.
14. J. Sun, L. Wu, Adsorption of protein onto double layer mixed matrix membranes, Colloids and surfaces. B, Biointerfaces, 123 (2014) 33-8.
15. M.M. Ž. Stankevičiūtė, A. Beganskienė, A. Kareiva, Sol-gel synthesis of calcium phosphate coatings on Ti substrate using dip-coating technique, Chemija, 24 (2013) 288-295.
16. D. Xiao, X. Zhou, H. Li, Y. Fu, K. Duan, X. Lu, X. Zheng, J. Weng, Fabrication of hollow hydroxyapatite particles assisted by small organic molecule and effect of microstructure on protein adsorption, Journal of the European Ceramic Society, 35 (2015) 1971-1978.
17. S.K. Swain, D. Sarkar, Study of BSA protein adsorption/release on hydroxyapatite nanoparticles, Applied Surface Science, 286 (2013) 99-103.
18. E. Bogya, M. Czikó, G. Szabó, R. Barabás, The red beetroot extract antioxidant activity and adsorption kinetics onto hydroxyapatite-based materials, Journal of the Iranian Chemical Society, 10 (2013) 491-503.
19. A.-C. Dancu, R. Barabas, E.-S. Bogya, Adsorption of nicotinic acid on the surface of nanosized hydroxyapatite and structurally modified hydroxyapatite, Central European Journal of Chemistry, 9 (2011) 660-669.
20. L. Gu, X. He, Z. Wu, Mesoporous hydroxyapatite: Preparation, drug adsorption, and release properties, Materials Chemistry and Physics, 148 (2014) 153-158.
21. L.J. del Valle, O. Bertran, G. Chaves, G. Revilla-López, M. Rivas, M.T. Casas, J. Casanovas, P. Turon, J. Puiggalí, C. Alemán, DNA adsorbed on hydroxyapatite surfaces, J. Mater. Chem. B, 2 (2014) 6953-6966.
22. F. Vázquez-Hernández, C. Mendoza-Barrera, V. Altuzar, M. Meléndez-Lira, M.A. Santana-Aranda, M. de la L. Olvera, Synthesis and characterization of hydroxyapatite nanoparticles and their application in protein adsorption, Materials Science and Engineering: B, 174 (2010) 290-295.

23. E. Skwarek, W. Janusz, D. Sternik, Adsorption of citrate ions on hydroxyapatite synthetized by various methods, Journal of Radioanalytical and Nuclear Chemistry, 299 (2013) 2027-2036.
24. F. Castro, A. Ferreira, F. Rocha, A. Vicente, J. António Teixeira, Characterization of intermediate stages in the precipitation of hydroxyapatite at 37°C, Chemical Engineering Science, 77 (2012) 150-156.
25. I. Mobasherpour, M.S. Heshajin, A. Kazemzadeh, M. Zakeri, Synthesis of nanocrystalline hydroxyapatite by using precipitation method, Journal of Alloys and Compounds, 430 (2007) 330-333.
26. G. With, H.J.A. Dijk, N. Hattu, K. Prijs, Preparation, microstructure and mechanical properties of dense polycrystalline hydroxy apatite, Journal of Materials Science, 16 (1981) 1592-1598.
27. R.B. E.S. Bogya, L. Bizo, V.R. Dejeu. *Preparation and characterization of silicate hydroxyapatites used for copper sorption*. in *11th International Conference and Exhibition of the European Ceramic Society*. 2009 Krakow, Poland.
28. R. Barabás, M. Czikó, I. Dékány, L. Bizo, E.S. Bogya, Comparative study of particle size analysis of hydroxyapatite-based nanomaterials, Chem. Pap., 67 (2013) 1414-1423.
29. D. Lahiri, S. Ghosh, A. Agarwal, Carbon nanotube reinforced hydroxyapatite composite for orthopedic application: A review, Mater. Sci. Eng. C. Mater. Biol. Appl., 32 (2012) 1727-1758.
30. E.-S. Bogya, R. Barabás, A. Csavdári, V. Dejeu, I. Bâldea, Hydroxyapatite modified with silica used for sorption of copper(II), Chem. Pap., 63 (2009) 568-573.
31. M. Jarcho, C.H. Bolen, M.B. Thomas, J. Bobick, J.F. Kay, R.H. Doremus, Hydroxylapatite synthesis and characterization in dense polycrystalline form, J. Mater. Sci., 11 (1976) 2027-2035.
32. A. Paz, D. Guadarrama, M. López, J. E. González, N. Brizuela, J. Aragón, A comparative study of hydroxyapatite nanoparticles synthesized by different routes, Química Nova, 35 (2012) 1724-1727.
33. S. V. Dorozhkin, Amorphous Calcium Orthophosphates: Nature, Chemistry and Biomedical Applications, International Journal of Materials and Chemistry, 2 (2012) 19-46.
34. S. Mukherjee, B. Kundu, S. Sen, A. Chanda, Improved properties of hydroxyapatite–carbon nanotube biocomposite: Mechanical, in vitro bioactivity and biological studies, Ceram. Int., 40 (2014) 5635-5643.
35. Z. Leilei, L. Hejun, L. Kezhi, F. Qiangang, Z. Yulei, L. Shoujie, A Na and Si co-substituted carbonated hydroxyapatite coating for carbon nanotubes coated carbon/carbon composites, Ceramics International, (2014)
36. A.E. Porter, N. Patel, J.N. Skepper, S.M. Best, W. Bonfield, Effect of sintered silicate-substituted hydroxyapatite on remodelling processes at the bone-implant interface, Biomaterials, 25 (2004) 3303-14.
37. E.L. Solla, F. Malz, P. González, J. Serra, C. Jaeger, B. León, The Role of Si Substitution into Hydroxyapatite Coatings, Key Eng. Mater., 361-363 (2008) 175-178.
38. L. Chen, C.Y. Tang, H.S.-l. Ku, C.P. Tsui, X. Chen, Microwave sintering and characterization of polypropylene/multi-walled carbon nanotube/hydroxyapatite composites, Composites Part B: Engineering, 56 (2014) 504-511.
39. J. Venkatesan, Z.-J. Qian, B. Ryu, N. Ashok Kumar, S.-K. Kim, Preparation and characterization of carbon nanotube-grafted-chitosan – Natural hydroxyapatite composite for bone tissue engineering, Carbohydr. Polym., 83 (2011) 569-577.
40. K. Grandfield, F. Sun, M. FitzPatrick, M. Cheong, I. Zhitomirsky, Electrophoretic deposition of polymer-carbon nanotube–hydroxyapatite composites, Surface and Coatings Technology, 203 (2009) 1481-1487.
41. K. Bleek, A. Taubert, New developments in polymer-controlled, bioinspired calcium phosphate mineralization from aqueous solution, Acta biomaterialia, 9 (2013) 6283-321.
42. M. Sadat-Shojai, M.T. Khorasani, E. Dinpanah-Khoshdargi, A. Jamshidi, Synthesis methods for nanosized hydroxyapatite with diverse structures, Acta biomaterialia, 9 (2013) 7591-621.
43. H. Zhou, J. Lee, Nanoscale hydroxyapatite particles for bone tissue engineering, Acta biomaterialia, 7 (2011) 2769-81.
44. S.H. Teng, E.J. Lee, B.H. Yoon, D.S. Shin, H.E. Kim, J.S. Oh, Chitosan/nanohydroxyapatite composite membranes via dynamic filtration for guided bone regeneration, Journal of biomedical materials research. Part A, 88 (2009) 569-80.
45. X. Du, Y. Chu, S. Xing, L. Dong, Hydrothermal synthesis of calcium hydroxyapatite nanorods in the presence of PVP, J. Mater. Sci., 44 (2009) 6273-6279.
46. M.J.A. Mijarsh, M.A. Megat Johari, Z.A. Ahmad, Effect of delay time and Na2SiO3 concentrations on compressive strength development of geopolymer mortar synthesized from TPOFA, Construction and Building Materials, 86 (2015) 64-74.

47. C. Shu, Y. Xianzhu, X. Zhangyin, X. Guohua, L. Hong, Y. Kangde, Synthesis and sintering of nanocrystalline hydroxyapatite powders by gelatin-based precipitation method, Ceramics International, 33 (2007) 193-196.
48. K. Sing, The use of nitrogen adsorption for the characterisation of porous materials, Colloids and Surfaces A: Physicochemical and Engineering Aspects, 187-188 (2001) 3-9.
49. J. Peña, I. Izquierdo-Barba, M.A. García, M. Vallet-Regí, Room temperature synthesis of chitosan/apatite powders and coatings, Journal of the European Ceramic Society, 26 (2006) 3631-3638.
50. T. Wang, A. Dorner-Reisel, E. Müller, Thermogravimetric and thermokinetic investigation of the dehydroxylation of a hydroxyapatite powder, J. Eur. Ceram. Soc., 24 (2004) 693-698.
51. G.M. Neelgund, K. Olurode, Z. Luo, A. Oki, A simple and rapid method to graft hydroxyapatite on carbon nanotubes, Mater. Sci. Eng. C. Mater. Biol. Appl., 31 (2011) 1477-1481.
52. Z. Zyman, D. Rokhmistrov, V. Glushko, Structural changes in precipitates and cell model for the conversion of amorphous calcium phosphate to hydroxyapatite during the initial stage of precipitation, J. Cryst. Growth, 353 (2012) 5-11.
53. C. Kailasanathan, N. Selvakumar, Comparative study of hydroxyapatite/gelatin composites reinforced with bio-inert ceramic particles, Ceramics International, 38 (2012) 3569-3582.
54. K. Pandi, N. Viswanathan, In situ precipitation of nano-hydroxyapatite in gelatin polymatrix towards specific fluoride sorption, International journal of biological macromolecules, 74C (2014) 351-359.
55. X. Pang, I. Zhitomirsky, Electrophoretic deposition of composite hydroxyapatite-chitosan coatings, Materials Characterization, 58 (2007) 339-348.
56. L. Wang, C. Li, Preparation and physicochemical properties of a novel hydroxyapatite/chitosan–silk fibroin composite, Carbohydrate Polymers, 68 (2007) 740-745.
57. N. Davidenko, R.G. Carrodeguas, C. Peniche, Y. Solis, R.E. Cameron, Chitosan/apatite composite beads prepared by in situ generation of apatite or Si-apatite nanocrystals, Acta biomaterialia, 6 (2010) 466-76.
58. S.P. Victor, C.P. Sharma, Development and evaluation of cyclodextrin complexed hydroxyapatite nanoparticles for preferential albumin adsorption, Colloids and surfaces. B, Biointerfaces, 85 (2011) 221-8.
59. X.Y. Lu, N.Y. Zhang, L. Wei, J.W. Wei, Q.Y. Deng, X. Lu, K. Duan, J. Weng, Fabrication of carbon nanotubes/hydroxyapatite nanocomposites via an in situ process, Appl. Surf. Sci., 262 (2012) 110-113.
60. T. Zhou, Effect of silane treatment of carboxylic-functionalized multi-walled carbon nanotubes on the thermal properties of epoxy nanocomposites, eXPRESS Polymer Letters, 4 (2010) 217-226.
61. P.N. Chavan, M.M. Bahir, R.U. Mene, M.P. Mahabole, R.S. Khairnar, Study of nanobiomaterial hydroxyapatite in simulated body fluid: Formation and growth of apatite, Materials Science and Engineering: B, 168 (2010) 224-230.
62. W. Zhang, Y. Chai, X. Xu, Y. Wang, N. Cao, Rod-shaped hydroxyapatite with mesoporous structure as drug carriers for proteins, Applied Surface Science, 322 (2014) 71-77.
63. T. Boix, J. Gomez-Morales, J. Torrent-Burgues, A. Monfort, P. Puigdomenech, R. Rodriguez-Clemente, Adsorption of recombinant human bone morphogenetic protein rhBMP-2m onto hydroxyapatite, Journal of inorganic biochemistry, 99 (2005) 1043-50.
64. J.W. Shen, T. Wu, Q. Wang, H.H. Pan, Molecular simulation of protein adsorption and desorption on hydroxyapatite surfaces, Biomaterials, 29 (2008) 513-32.
65. R.C.H. Diana T. Hughes Wassell, Graham Embery, Adsorption of bovine serum albumin onto hydroxyapatite, Biomoterials, 16 (1995) 697-702.
66. E. Fujii, M. Ohkubo, K. Tsuru, S. Hayakawa, A. Osaka, K. Kawabata, C. Bonhomme, F. Babonneau, Selective protein adsorption property and characterization of nano-crystalline zinc-containing hydroxyapatite, Acta biomaterialia, 2 (2006) 69-74.
67. N. Zhang, T. Gao, Y. Wang, Z. Wang, P. Zhang, J. Liu, Environmental pH-controlled loading and release of protein on mesoporous hydroxyapatite nanoparticles for bone tissue engineering, Materials science & engineering. C, Materials for biological applications, 46 (2015) 158-65.
68. Y.K. Tovbin, Foundations of the fluctuation theory of adsorption on microcrystalline particles, Russian Journal of Physical Chemistry B, 4 (2011) 1033-1045.
69. T. Kokubo, H.-M. Kim, M. Kawashita, Novel bioactive materials with different mechanical properties, Biomaterials, 24 (2003) 2161-2175.
70. E. Chevalier, M. Viana, S. Cazalbou, L. Makein, J. Dubois, D. Chulia, Ibuprofen-loaded calcium phosphate granules: combination of innovative characterization methods to relate mechanical strength to drug location, Acta biomaterialia, 6 (2010) 266-74.

71. L.G. Bach, M.R. Islam, K.T. Lim, Expanding hyperbranched polyglycerols on hydroxyapatite nanocrystals via ring-opening multibranching polymerization for controlled drug delivery system, Materials Letters, 93 (2013) 64-67.
72. C. Zhang, C. Li, S. Huang, Z. Hou, Z. Cheng, P. Yang, C. Peng, J. Lin, Self-activated luminescent and mesoporous strontium hydroxyapatite nanorods for drug delivery, Biomaterials, 31 (2010) 3374-83.
73. J. Andersson, J. Rosenholm, M. Linden, *Mesoporous silica: An alternative diffusion controlled drug delivery system*, in *Topics in Multifunctional Biomaterials & Devices*.
74. C.S. M. Betsiou, A. Papageorgiou, Adsorption of Oxaliplatin by Hydroxyapatite, Bioautomation, 8 (2007) 138-145.
75. J.K. Pattarawadee Phichetbovornkul, Lupong Kaewsichan. *Development of Hydroxyapatite-Chitosan Matrix as a Drug Carrier*. in *The 10th International PSU Engineering Conference*. 2012. Hat Yai, Thailand.
76. H. Yang, L. Hao, N. Zhao, C. Du, Y. Wang, Hierarchical porous hydroxyapatite microsphere as drug delivery carrier, CrystEngComm, 15 (2013) 5760.

Scientific papers - articles

1. **E.-S. Bogya, M. Czikó, G. Szabó, R. Barabás:** *The red beetroot extract antioxidant activity and adsorption mechanism onto hydroxyapatite-based materials,* Journal of the Iranian Chemical Society, pp. 491-503*,* **2013.** DOI: 10.1007/s13738-012-0183-3**,** *impact factor* - **1.406**
2. **R. Barabás, M. Czikó, I. Dékány, L. Bizo, E. S. Bogya***: Comparative study of particle size analysis for hydroxyapatite-based nanomaterials,* Chemical Papers 67 (11), pp. 1414-142, **2013**. DOI: 10.2478/s11696-013-0409-6*, impact factor* - **1.096**
3. **M. Czikó, E. S. Bogya, R. Barabás, L. Bizo:** *In vitro biological activity comparison of some hydroxyapatite-based composite materials using simulated body fluid*, Central European Journal of Chemistry, 11 (10), pp. 1583-1598, **2013**. DOI: 10.2478/s11532-013-0293-5, *impact factor* - **1.329**
4. **E. S. Bogya, M. Czikó, R. Barabás, A. Csavdári:** *Influence of synthesis method of nano-hydroxyapatite based materials on cadmium sorption processes*, Journal of the Iranian Chemical Society*, Volume 11 (1),* pp. 53-68*,* **2014.** DOI: 10.1007/s13738-013-0275-8, *impact factor* - **1.406**
5. **M. Czikó**, **E. S. Bogya, M. V. Diudea, R. Barabás:** *Research on hydroxyapatite based composite materials* - Revue Roumaine de Chimie, *59(5)*, pp. 353-357, **2014.** *impact factor* – **0.393**
6. **R. Barabás, G. Katona, E. S. Bogya, M. V. Diudea, A. Szentes, B. Zsirka, J. Kovács, L. Kékedy-Nagy, M. Czikó**: *Preparation and characterization of carboxyl functionalized multiwall carbon nanotubes-hydroxyapatite composites,* -Ceramics International, - submitted, *impact factor* - **2.086**

Scientific communications

1. **M. Czikó, E.S. Bogya, R. Barabás, L. Bizo,** *Hydroxyapatite composites particle size changes with time*, XVII. International Conference on Chemistry, 23. page, Cluj Napoca, s**03.11.2011-** *presentation*
2. **M. Czikó, R. Barabás, L. Bizo, E.S. Bogya,** Testing of hydroxyapatite based materials behavior in water and in SBF**,** *XVIII. International Conference on Chemistry, pag. 23, Băile Felix,* ***23.11.2012*** *- presentation*

3. **M. Czikó, E.S. Bogya, R. Barabás, G. Katona, A. Szentes,** Testing of Carbon nanotubes/Hydroxyapatite/Ibuprophen behavior in simulated body fluid, Conference of „Environment friendly materials and technologies" and 56th "Hungarian Spectroscopy Symposium, Hungary, Veszprém, **01-03.07. 2013** - *poster*
4. **M. Czikó, R. Barabás, E.S. Bogya, G. Katona,** Preparation and examination of hydroxyapatite based composites, XIX. International Conference on Chemistry, pag. 39, Baia Mare, **21-23. 11. 2013**. - *presentation*
5. **M. Czikó, R. Barabás, E.S. Bogya, G. Katona,** Preparation and Characterization of Hydroxyapatite-carbon nanotubes biocomposites, PhD Conference, Szeged, Hungary, **01.03.2014** - *presentation*
6. **M. Czikó, E.S. Bogya, R. Barabás,** Nano-hydroxyapatite based materials synthesis method influence on Cd^{2+} sorption mechanism, 4th International Conference Natura – Econ, Sfantu Gheorghe, **07.03.2014** - *poster*
7. **M. Czikó, R. Barabás, E.S. Bogya,** Preparation and characterization of hydroxyapatite based biomaterials, Jedlik Ányos professional days, Veszprém, Hungary, **11-13. 04. 2014** - *poster*
8. **M. Sárközi, B. Csákány, R. Barabás, G. Katona, E.S. Bogya**, Albumine adsorption study on hydroxyapatite based composites, XX. International Conference on Chemistry, page 39, Cluj Napoca, **6-9.11.2014** - *presentation*